ABSTRACT

Preparation of Two Step Thermo-Responsive Membrane with Tunable Separation Property and Improved Cleaning Efficiency

Choi Jung-Yun

Department of Materials Science and Engineering

The Graduate School

Seoul National University

We developed the two step thermo-responsive membrane with tunable selectivity and improved cleaning efficiency by introducing thermo-responsive block copolymer. To achieve this, we prepared poly (N, N-dimethylamino ehtylmethacrylate)-b-poly (N-isopropyl acryl-amides) (PDMAEMA -b-PNIPAM, PDN) which have two different lower critical solution temperature (LCST) behaviors. The two step

thermo-responsive membrane (PES/PDN) was prepared with blending PDN block copolymer and poly (ether sulfone) by phase inversion method. Fourier transform infrared (FT-IR) and proton nuclear magnetic resonance (^{1}H NMR) analysis identified that PDN block copolymers are successfully synthesized. Two step thermo-responsibility of PDMAEMA-b-PNIPAM was determined by proton nuclear magnetic resonance (^{1}H NMR), dynamic light scattering (DLS). 1st aggregation occurred at 40 ℃, and then 2nd aggregation occurred at 40-60 ℃. Furthermore, successful preparation of PES/PDN membrane was confirmed by attenuated total reflectance Fourier transform infrared (ATR/FT-IR) and X-ray photoelectron spectroscopy (XPS) analysis. Finally, filtration tests and fouling tests were carried out in order to demonstrate the tunable separation property and improved cleaning efficiency of the membrane. As expected, the PES/PDN membrane showed two step transition of permeability and rejection property at 40 ℃ and 50-70 ℃. Likewise, cleaning efficiency of membrane increased when cleaning temperature is at 60 ℃ than at 30 ℃. Therefore we demonstrated that two step thermo-responsive membrane was successfully prepared, and it could control the separation property and improve cleaning efficiency.

Keywords

Ultrafiltration, Stimuli responsive membrane, Thermo-responsive membrane, PNIPAM, PDMAEMA, Pore size control, Tunable separation property, Cleaning efficiency

***Student Number*: 2014-21491**

Table of Contents

1. Introduction

In recently, membrane techniques have been widely interested in environmental and biochemical applications. Membranes separate different molecules by size exclusion methods, and classified into reverse osmosis (RO), nanofiltration (NF), ultrafiltration (UF) and microfiltration (MF) according to pore size. Especially, ultra/micro filtration (UF/MF) membranes have relatively large pore size, and usually separate various type of materials such as proteins, viruses, and food waste. Thus, UF/MF membranes are generally used in separation process such as water treatment, and membrane bioreactor (MBR) because of their simple operation and inexpensive costs than other methods [1, 2].

Unfortunately, UF/MF membranes still have the problem that once fabricated membranes show restricted separation property due to their fixed pore size. When the size of aimed molecules are different, a new type of membrane with proper pore size is needed in order to keep a high separation property. Moreover, since UF/MF membrane's materials such as polysulfone (PSF), polyether sulfone (PES), and polyvinylidene fluoride (PVDF) are usually hydrophobic, membranes

are easy to be contaminated by hydrophobic pollutants like proteins, nature organic materials or others. In order to solve the fouling issue, many researches were performed to give hydrophilicity at membrane surface by various surface modification methods [3, 4]. Those researches are focused on delaying the fouling late. However, the membrane still need additional cleaning process because it must be eventually fouled. Thus, researches about developing efficient cleaning methods are emerging issues for membrane process.

Lately, stimuli-responsive membranes have been widely interested in order to improve the existing issues of UF/MF membranes. Stimuli-responsive membranes are membranes that can change the various surface properties in response to the external stimulus such as temperature, pH, electrolyte, magnetic field, and light [5-8]. Therefore, stimuli-responsive membrane could change their pore size and hydrophilicity by the external stimulus, and could be used in various application with these properties. The stimuli-responsive behaviors are obtained by introducing stimuli-responsive materials near the membrane surface by grafting or blending methods [9]. Normally stimuli-responsive materials, also called as smart materials, have special functional groups within or on a polymer chain, and able to

shrink or expand, to change their optical properties depending on environmental changes. The typical examples of stimuli-responsive materials are shown in figure 1 [10]. Therefore, when those polymers are introduced in membrane by grafting or blending methods, the surfaces can change their wettability and permeability, as well as their adhesive, adsorptive, mechanical and optical properties [11]. Particularly, when stimuli-responsive materials have volume transition properties, membranes could control the pore size, which can role as gating membranes [12].

Among the various type of stimulus, temperature is mainly considered for preparing stimuli-responsive membranes. Because temperature is easy to control and do not affect the component of solution, thermo-responsive membranes are adequate for membrane applications. Usually thermo-responsive polymers have own LCST (Lower critical solution temperature) or UCST (Upper critical solution temperature) temperatures. Above those temperature, polymer structure altered from randomly stretched structure to coil structure due to the solubility difference under the aqueous solution. Therefore, volume and hydrophilicity of thermo-responsive polymers could be changed in relation to the temperature transition. For example, the PNIPAM, one

of the most well-known thermo-responsive polymer, has the 32 ℃ of LCST, and the volume of polymer decreases above the temperature because its hydrogen bonding with water molecules breaks above the temperature and form coiled structure [13]. Consequently, when the PNIPAM exists near the membrane surface or pore, polymer brushes can close or open the pore by the volume transition. By taking advantages of these principles, thermo-responsive membranes have been used in various application such as biosensor [14, 15], drug delivery [16], tissue engineering [17], and separation process.

Specifically in separation process, thermo-responsive membranes have two important advantages than normal ultrafiltration membranes. First of all, permeability and separation property of membrane is controlled by temperature variation due to the pore size transition. Thus, the kinds of filtered materials could be controlled by temperature. Jing-Zhen et al. prepared membranes with PNIPAM grafted PVDF copolymers, and verified the size of filtrated Fe_2O_3 particles was different at 25 ℃ and 40 ℃ [18]. Similarly, Chen Xi et al. prepared membranes by phase inversion of mixture of PNIPAM microgels and PVDF, and identified the change of permeability and BSA rejection ratio at increased temperature [19]. Li Qian et al. immobilized the poly

(3-(methacryloylamino) propyldimethyl-(3-sulfo propyl) ammonium hydroxide) (PMPDSAH) on the PVDF membranes via grafting polymerization, and observed the MWCO alteration at different temperature [20].

Meanwhile, there are researches that focused on the anti-fouling and efficient cleaning of thermo-responsive membrane. Based on the principles that back-washing efficiency increased at large pore size, Yu Sanchuan et al. modified the membranes by depositing P(NIPAM-co-AM) and confirmed that membrane performance was recovered well when cleaning at 45 ℃ than cleaning at 30 ℃ [21, 22]. There is another way to improve cleaning efficiency. Sinha M. K., and M. K. Purkait prepared a novel thermo responsive PSF membrane with cross linked PVCL-co-PSF. They found that foulants were physically eluted from membrane surface when cleaned at alternate temperature-change caused by the reversible volume phase transition of PVCL [23, 24].

Recently, dual thermo-responsive block copolymers are discussed widely due to their potential application in drug delivery, biological separation and tissue engineering. When block copolymers having two different LCSTs behaviors, structure of one block collapses at the first transition temperature, and transform the hydrophilic polymer to an

amphiphilic one. Thus, these amphiphilic block copolymers can have self-assembly property and reversibly form various structure like micelle or vesicles. Also when heating the polymer beyond the second transition temperature, other blocks also collapse, thus finally hydrophilic polymer converts into hydrophobic polymer [25]. For instance, PNIPAM-b-PDMAEMA [26, 33], P(DMAEMA-b-DEGMA) [27], PNIPAAm-b-P(NIPAAm-co-HEAAm)) [28], and PNPAM-b-PNEAM [29] are prepared by living polymerization methods such as ATRP and RAFT. Because there are lots of types of thermo-responsive polymers, we could control the phase transition properties by choosing the suitable thermo-responsive polymers.

In this work, we prepared the two step thermo-responsive membranes which have two different LCST behaviors. Two step thermo-responsive membranes show more various transition than existing thermo-responsive membranes, so it could be separate more various materials also with improved cleaning efficiency. In order to realize the two step thermo-responsibility, we mixed the polyethersulfone (PES) membrane with two different thermo-responsive polymers. Among the block copolymer as mentioned above, PNIPAM-b-PDMAEMA block copolymer was selected as materials for

two step thermo-responsive membrane. [33] As mentioned above, PNIAPM has the LCST at 32 ℃ which is close to body temperature and easy to applicate in versatile field [13, 30]. Moreover, in case of PDMAEMA, LCST changes in various range by degree of polymerization (DP). Therefore, we could control the LCST range appropriately for various applications [31]. In these principles, two step thermo-responsive could be used in separation process such as food process. For example, food waste contains various nutraceuticals such as sugars (< 1kDa), whey proteins (25 kDa), or β-glucan (50 kDa), and it needs to be separated. Finally we prepare PES/PDN membrane by phase inversion methods, and evaluate the two step thermo-responsibility with filtration property and cleaning performance.

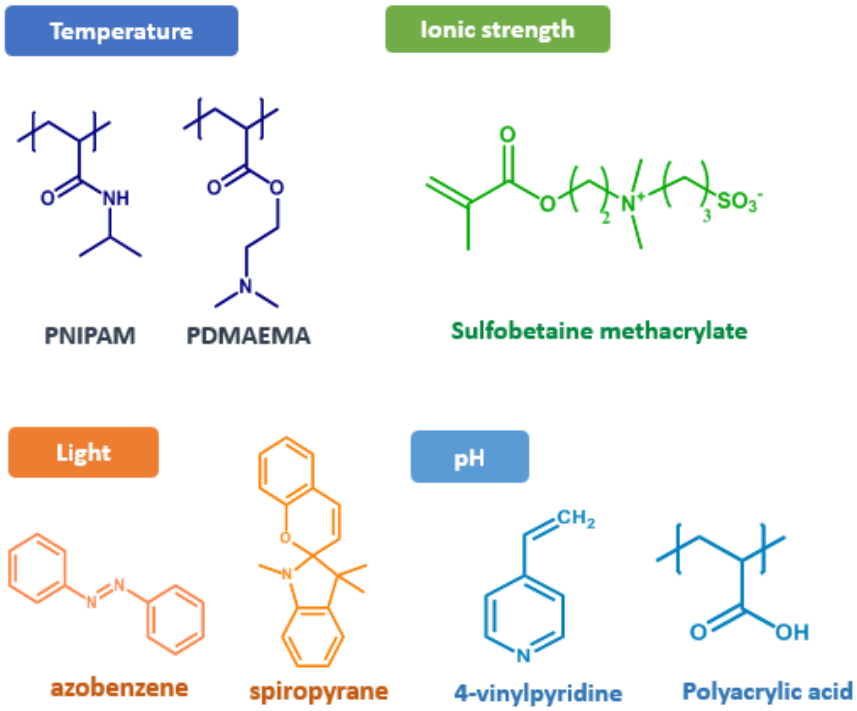

Figure 1. Types of various stimuli-responsive materials

2. Experimental section

2.1. Materials

1-Dodecanthiol (98%, Daejung), Sodium hydride (60% dispersion in mineral oil, Daejung), Ethyl ether (99%, Daejung), Carbon disulfide (99%, Daejung), Iodine (solid, 99%, Daejung), 4,4'-azobis(4-cyanopentanoic acid) (≥98%, Aldrich) were used to synthesize RAFT agent of 4-cyano-4-(dodecylsulfanylthiocarbonyl) sulfanyl pentanoic acid (CDTPA). The monomer of N-isopropylacrylamide (NIPAM, ≥99%, Aldrich), 2-Dimetylaminoethyl methacrylate (DMAEMA, 98%, Aldrich) were used as temperature responsive polymers. 2,2'-Azobis(2-methylpropionitrile) (AIBN, extra pure, Daejung) were used as initiator. Poly ether sulfone (PES) was selected as materials for membrane. Polyvinylpyrrolydone (PVP, Daejung) was used as pore forming agent. Globulin, Bovine serum albumin (BSA), Lysozyme, Hemoglobin (Hb) were purchased from Sigma-Aldrich, and used as pollutants for filtration tests.

2.2. Synthesis of PDMAEMA-b-PNIPAM block copolymer

2.2.1 Synthesis of RAFT agent [4-cyano-4-(dodecylsulfanyl thiocarbonyl) sulfanyl pentanoic acid]

For the first step, the synthesis of CDTPA was conducted according to a previously reported method [32], and overall scheme is described at figure 2. Sodium hydride (3.15 g, 79 mmol) suspension in diethyl ether (150 mL) was stirred 10 min at 5-10 ℃. Then, n-Dodecylthiol (15.4 g, 76 mmol) was added to the suspension, which made sodium hydride transformed to white slurry of sodium thiododecylate. The reaction mixture was cooled to 0 ℃ and added carbon disulfide (6.0 g, 79 mmol). Then a yellow precipitate of S-dodecyl trithiocarbonate* was collected by filtration.

* FT-IR spectra: 1200-1050 cm^{-1} (C=S), 750-700 cm^{-1} (C-S), 680-610 cm^{-1} (Sulfate ion)

As the second step, Iodine (6.3 g, 25 mmol) was added to a suspension of S-dodecyl trithiocarbonate (14.6 g, 49 mmol) in diethyl ether (100 mL). The reaction mixture was stirred for 1 h at room temperature. After the reaction, the excess iodine was removed by

filtration.

Then, filtrate was washed by sodium chloride solution (1M) by separating funnel to remove excess iodine, and dried with sodium sulfate to remove water. Finally, bis-(dodecyl-sulfanylthiocarbonyl) disulfide* was obtained by evaporating.

* FT-IR spectra: 1600-1450 cm^{-1} (S-S)

At final step, a mixture of bis-(dodecyl-sulfanylthiocarbonyl) disulfide (2.77 g, 5 mmol) and 4,4'-azobis(4-cyanopentanoic acid) was dissolved in ethyl acetate (50 mL). The solution was reacted with reflux at 70 ℃ for 18 h. The final product (4-cyano-4-(dodecylsulfanyl thiocarbonyl) sulfanyl pentanoic acid)* was precipitated in water and dried under vacuum overnight.

* FT-IR spectra: 1640-1575 cm^{-1} (N=N), 2260-2210 cm^{-1} (CN), 1750-1735 cm^{-1} (C=O), 3400-2400 cm^{-1} (OH)

The FT-IR results of each steps are presented at figure 3.

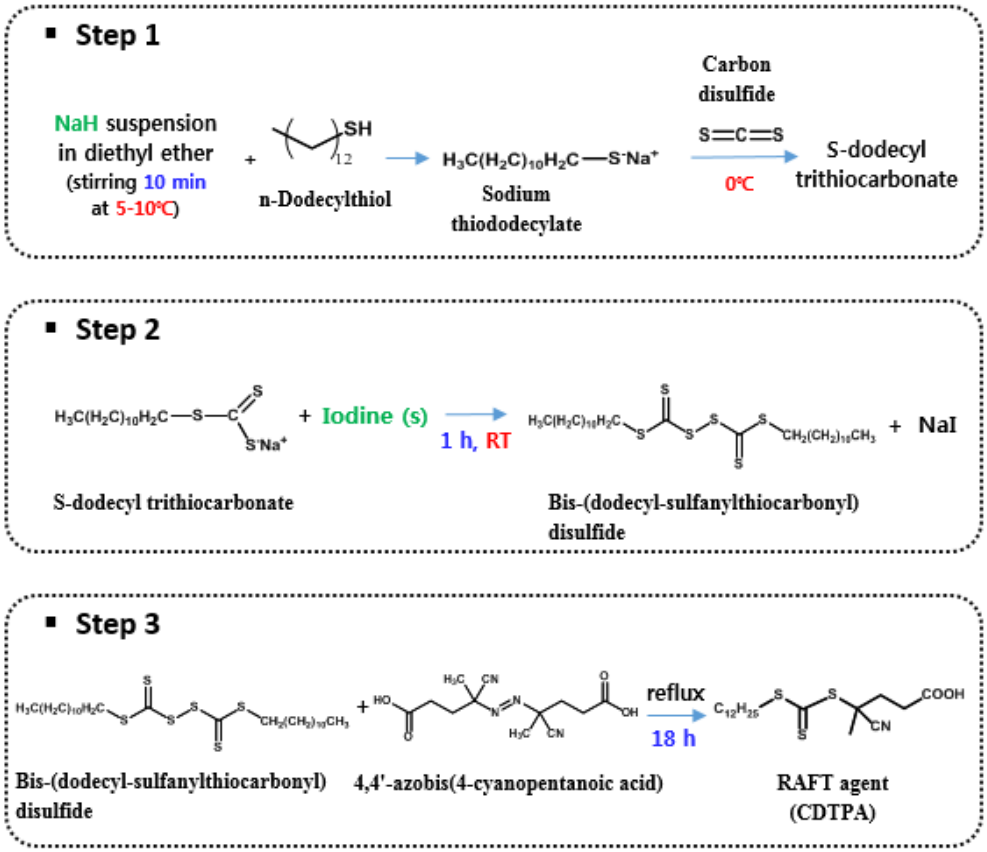

Figure 2. Synthesis of RAFT agent [4-cyano-4-(dodecylsulfanyl thiocarbonyl) sulfanyl pentanoic acid, CDTPA]

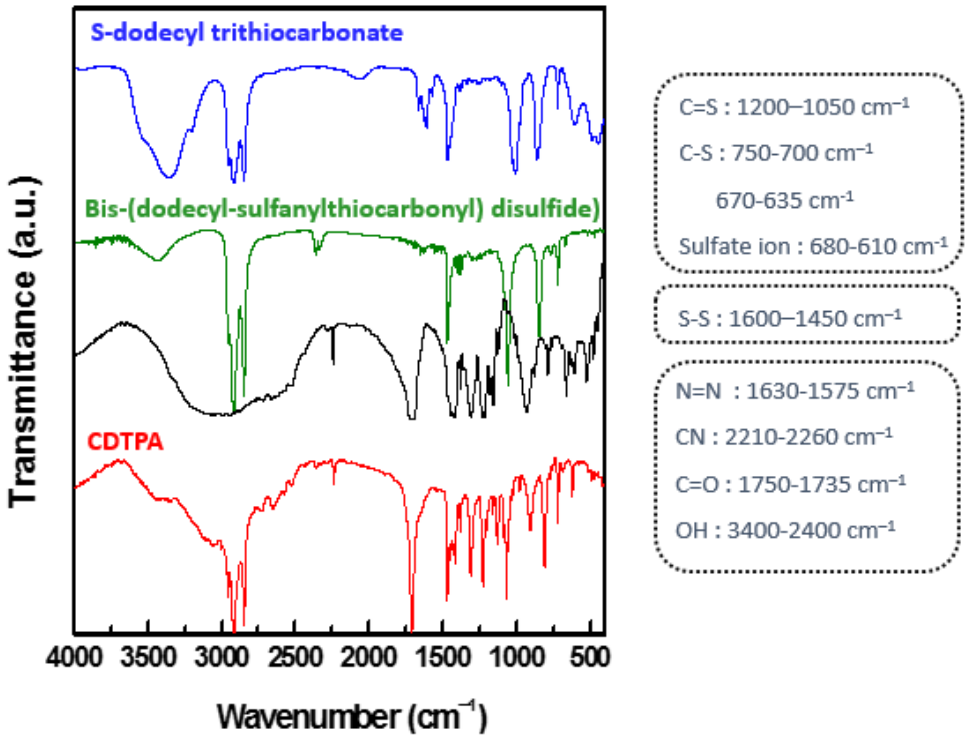

Figure 3. FT-IR spectra of CDTPA

2.2.2 Polymerization of PDMAEMA-b-PNIPAM

The PDMAEMA-b-PNIPAM block copolymer was synthesized by solution RAFT polymerization [33]. Into a 50 mL flask, DMAEMA (6.28 g, 40mmol), CDTPA (0.21 g, 0.51 mmol), AIBN (25.7 mg, 0.17 mmol) were dissolved in 1,4-dioxane (7.2 g). The solution was purged with nitrogen in order to remove oxygen and water at 0 ℃ for 30 min, and then polymerized at 70 ℃ for 5 h. Then, the flask was rapidly immersed into iced water to terminate polymerization. The yellow sticky polymer was obtained after precipitating in iced n-hexane, and final product was washed and dried under vacuum at room temperature overnight. (5.0 g, yield: 77%)

The synthesized polymer PDMAEMA (3.33 g, 0.36 mmol) was dissolved with NIPAM (3.62 g, 32 mmol), AIBN (19.2 mg, 0.12 mmol) in 1, 4-dioxane (18.0 g). The solution was purged with nitrogen at 0 ℃ for 30 min, and then polymerized at 65 ℃ for 2.5 h. Then, the flask was rapidly immersed into iced water to terminate polymerization. The synthesized PDMAEMA-b-PNIPAM (PDN) diblock copolymer was purified in n-hexane at 0 ℃, and dried under vacuum at room temperature overnight. (4.97 g, yield: 71%). The overall scheme of the reaction was presented in figure 4.

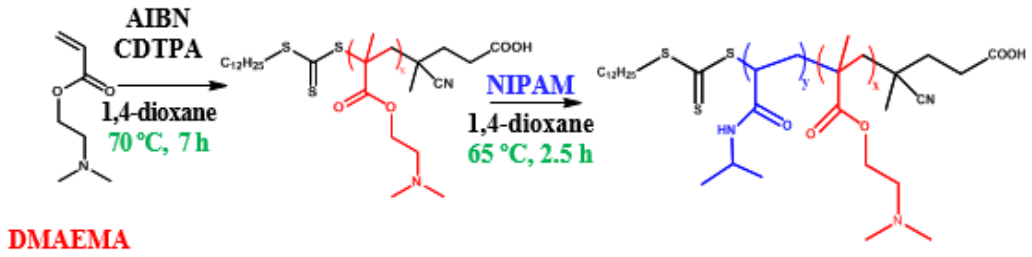

Figure 4. Polymerization of PDMAEMA-b-PNIPAM (PDN)

2.3. Preparation of PES/PDN membrane

PES/PDN membrane was prepared by phase inversion from DMSO dope solutions. The dope solution was prepared by blending with 15 wt. % of PES, 2 wt. % of PVP, and 0, 5, 10 wt. % of PDN block copolymer at 50 ℃ for 5 h. (PVP play a role to form enough pore at PES membrane.) The concentration of each sample was shown in table 1 [34, 35]. The dope solution was cast on a glass plate using a doctor blade with uniform thickness of 50 μm. Then the casted membrane was immersed into de-ionized water at room temperature. During the phase inversion, the RAFT agent end groups were anchored with PES matrix, and hydrophilic PDMAEMA and PNIPAM blocks are get out from matix. To remove the excess solvent, the fabricated membranes were kept in fresh DI water for overnight. The overall steps are shown in figure 5.

Table 1. Sample code and weight percent (wt. %) of PES, PDN, PVP, DMAc

Membrane code	PES (wt%)	PDN (wt% relative to PES)	PVP (wt%)	DMAc (wt%)
Neat-PES	15	0	2	85
PES/PDN5		5		
PES/PDN10		10		

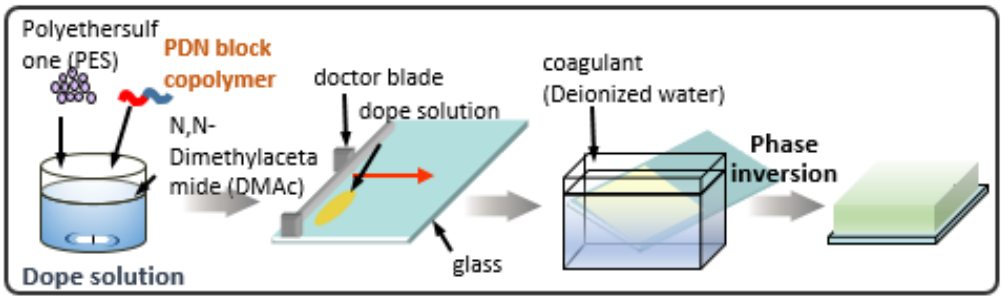

Figure 5. Preparation of PDN blended PES membrane by phase inversion methods

2.4. Characterization

2.4.1 Analysis of chemical structure of PDN block copolymer

The chemical structure of PDN block copolymer was analyzed by Fourier transform infrared (FT-IR, Thermo Scientific Nicolet iS5) spectroscopy and proton nuclear magnetic resonance (^{1}H NMR, Bruker AVANCE 600) spectroscopy in $CDCl_3$. Molecular weight of the polymer was calculated by ^{1}H NMR analysis by comparing integral ratio of RAFT agent peak and polymer block peak.

2.4.2 LCST confirmation of PDN block copolymer

The ^{1}H NMR analysis (Bruker AVANCE 600) of the polymer dissolved in D_2O was performed at different temperature to determine the LCST. Above the LCST, the main peaks of PNIPAM and PDMAEMA were disappeared due to the solubility difference of PDN block copolymer with water. The analysis was completed from 30 ℃ to 70 ℃ at intervals of 5 ℃.

In order to determine the volume transition rate of PDN block copolymer, 1mg/mL concentration of PDN block copolymer was dissolved in de-ionized water, and then analyzed by Dynamic light scattering (DLS, ELS-8000) analysis. The hydrodynamic size was observed at every 1 ℃ from 30 ℃ to 80 ℃, and equilibrium time was 2 min.

2.4.3 Membrane characterization

The presence of PDN block copolymer in prepared membrane was characterized by attenuated total reflection Fourier-transform infrared (ATR/FT-IR, Thermo Scientific Nicolet iS5) spectroscopy. The X-ray photoelectron spectroscopy (XPS, KRATOS AXIS- His) analysis using Mg Kα was done to identify the concentration of PDN block copolymer on membrane surface. Atomic concentration of carbon, nitrogen, sulfur, and oxygen was observed by XPS analysis.

In order to observe the morphologies of the membranes, both surface and cross-section of the membranes was analyzed by scanning electron microscope (SEM, JEOL JSM-7600). To obtain the cross-section sample, the membranes were frozen at liquid nitrogen, and broken. Then both samples were attached to supports, and dried for overnight.

Hydration capacity, the amount of absorbed water per unit volume [$mg \cdot cm^{-3}$], was determined by the following method. [23] First of all, membrane sample was prepared as 2 cm^{-1} size, and then weight was measured in dry state. Next, each sample was wetted in water for different temperature (30, 45, 60 ℃) for above 12 hours. Finally weight of membrane in wet state was measured after eliminating the surface water with towels. The weight difference of membrane in dry state and wet state was divided by volume of membrane. The thickness of membrane was figured out by coolant proof micrometer (mitutoyo). The experiments are repeated for 5 different samples for each membrane, and average value was used to roughly compare the porosity transition.

2.5. Membrane performance evaluation

2.5.1 Pure water permeation and filtration experiments

The membrane filtration experiments were performed with ultrafiltration system which was composed of 10 mL stirred cell (Amicon® 8010) connected to a pressure vessel with a pressure gauge (Millipore Corp.) as shown in figure 6. The effective membrane area of the cell was 4.91 cm^2.

So as to figure out the water flux transition on temperature variation, the reservoir was filled with pure de-ionized water, and filtration test was performed at 1.2 bar until the water flux was saturated (about 10-20 min). During the filtration, the weight difference of filtrated water was recorded for every 10 seconds by an electronic balance (CUW4200H, CAS corp.). The filtration test was repeated at different temperature (30, 35, 42, 50, 60, 70 ℃). Then the average pure water flux (PWF) of each temperature was calculated by equation (1).

$$J_w = \frac{V}{A\Delta t} \qquad (1)$$

J_w is pure water permeability (L/m^2h), V is the volume of filtrated water (L), A is the effective membrane area (m^2), and Δt is permeation time

(h).

To evaluate the tunable separation property of the membrane, rejection test for different solutes was performed. Globulin (92 kDa), BSA (66 kDa), Lysozyme (16 kDa) which showed size difference was selected as filtered materials, and then we observed the change of permeation ratio at different temperature. First of all, the protein solution (1000 ppm) of each sample was prepared as feed solution and then filtrated by ultrafiltration system at 1.2 bar. After passing the initial filtrate for 3 minute, filtrate was collected in centrifuge tube. The same process was repeated at 30-70 ℃. The concentration of proteins in filtrated solution was estimated by UV-visible spectrophotometer (Perkin Elmer, Lambda 25) at wavelength of 280 nm. Finally, permeation ratio of each proteins were calculated by following equation:

$$P(\%) = \left(\frac{C_{permeate}}{C_{feed}}\right) \times 100 \qquad (2)$$

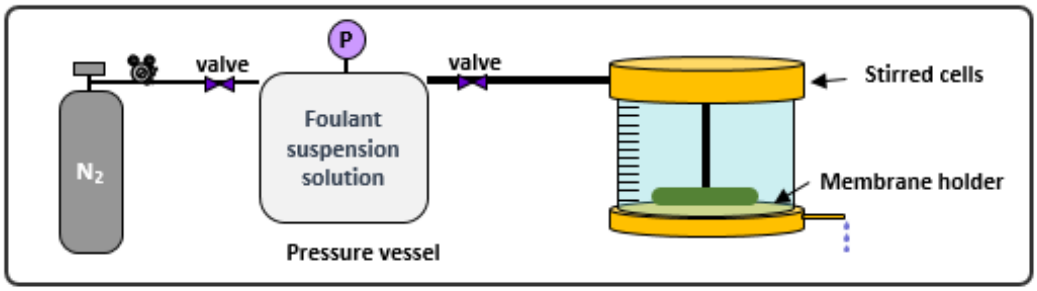

Figure 6. Schematic illustration of membrane performance evaluation system

2.5.2 Evaluation of fouling resistance

The fouling resistance and the cleaning efficiency of the membrane were identified by the following filtration experiments. And during the filtration, the corresponding water flux was recorded by an electronic balance (CUW4200H, CAS corp.). First of all, pure de-ionized water was permeated for 30 min, and corresponding flux was called as J_0. Then hemoglobin solution (500 ppm) was permeated until the water flux was saturated (for about an hour, called as J_P) in order to contaminate the membrane. After that, the fouled membrane was cleaned by back-washing process for 30 min, and the pure water flux was observed again (J_R). A back- washing process was performed respectively at 30 ℃ and 60 ℃ in order to compare the cleaning efficiency at each temperature. Repeat the same process for every sample, and compare the flux recovery ratio (FRR %), and reversible-irreversible fouling resistance.

3. Results and discussion

3.1. Preparation of PDMAEMA-b-PNIPAM (PDN)

Polymerization of PDN was conducted by solution RAFT polymerization, and the results were identified with FT-IR and ^{1}H NMR analysis.

The FT-IR spectra is represented in figure 7. The most important change after polymerization of PD (PDMAEMA) is that the C=C double bond peak at 1650-1630 cm^{-1} is disappeared, which verifying that almost all of the DMAEMA monomers are converted to polymers. In addition, the peaks at 1750 cm^{-1} and 1210-1150 cm^{-1} due to C=O and C-N group still observed after polymerization. As expected, the main peaks of NIPAM monomers such as N-H peak (3360-3310 cm^{-1}) and amide peak (1700-1630 cm^{-1}, 1560-1540 cm^{-1}) appeared together after PDN block copolymerization.

Figure 8 shows the ^{1}H NMR spectra of monomers and polymers. The main peaks of DMAEMA (B, C, D, E) and NIPAM (c, d) monomer chains are still observed after polymerization.

Furthermore, spectrum of PD exhibits the end group of CDTPA peaks at i (δ=0.89ppm) and j (δ=1.24 ppm). Thus, we confirmed that PDN copolymer was successfully synthesized with CDTPA end group.

According to the integral ratio of j peak (δ=1.24 ppm, terminal of RAFT agent) and D peak (δ=2.29 ppm, PDMAEMA), the degree of polymerization (DP) of PD was calculated to 53. Similarly, using the equation (3) the DP_{NIPAM} was calculated as 40. Finally, DP and related molecular weight was notified at table 2.

$$DP = \frac{[\text{intensity of (B+c)-C}]}{[\text{C peak intensity}]/\ [2 \times DP_{PDMAEMA}]} \qquad (3)$$

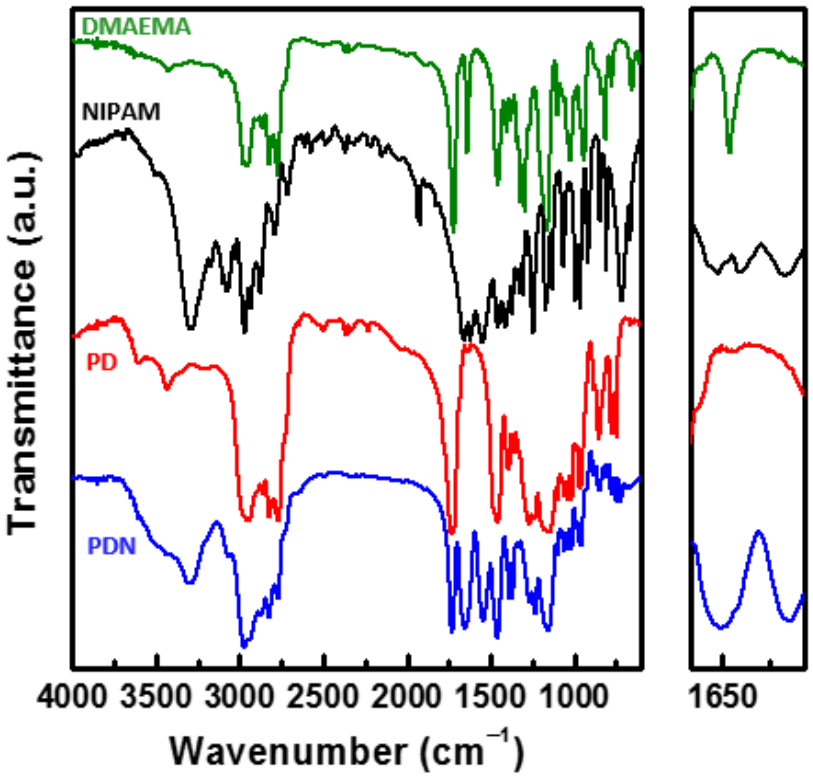

■ **DMAEMA**

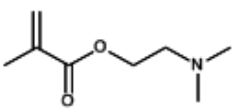

C=O : 1760-1740 cm^{-1}

C=C : 1650–1630 cm^{-1}

C-N : 1210-1150 cm^{-1}

■ **NIPAM**

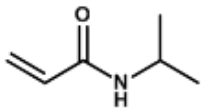

N-H : 3360-3310 cm^{-1}

Amide I : 1700-1630 cm^{-1}

Amide II : 1560-1540 cm^{-1}

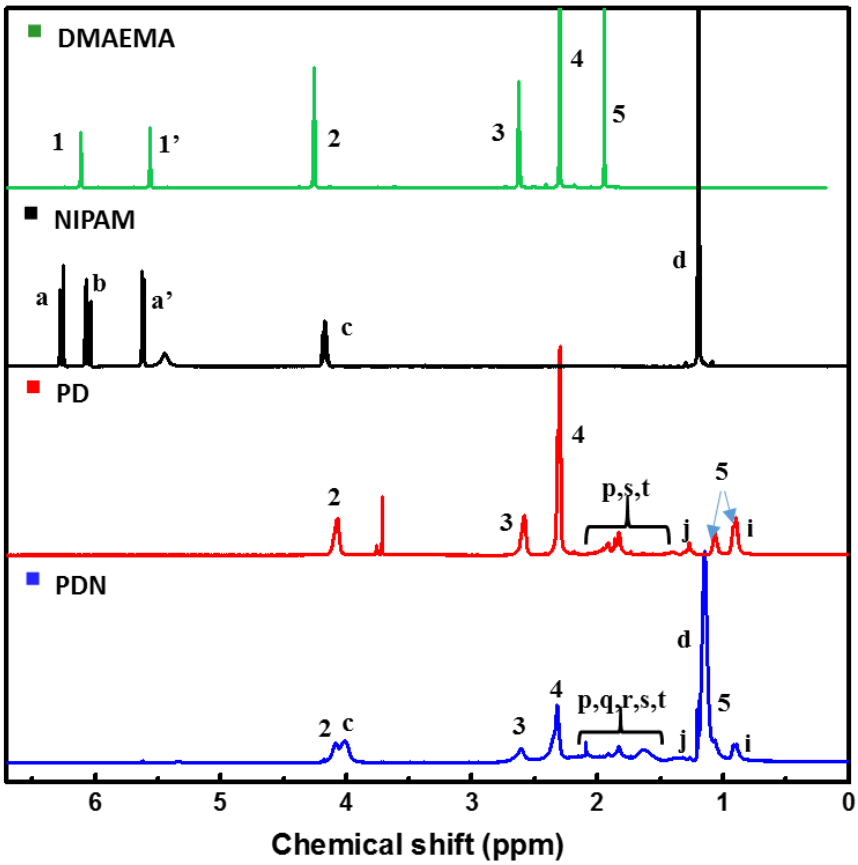

Figure 8. ^{1}H NMR spectra of DMAEMA, NIPAM, PD, PDN

Table 2. Degree of polymerization (DP) and molecular weight (MW) calculated by ^{1}H NMR results

^{1}H NMR							
Sample code	[RAFT agent]/ [Monomer]	DP_n				$M_{n,\ ideal}$ (g/mol)	$M_{n,\ NMR}$ (g/mol)
		ideal		NMR			
PD	1 : 80	68		53		11093.9	8735.8
PDN	1 : 66	PD	PN	PD	PN	14620.1	13262.2
		53	52	53	40		

3.2. Two step thermo-responsive behavior of PDN block copolymer

3.2.1 LCST confirmation of PDN block copolymer

The PDMAEMA-b-PNIPAM diblock copolymers contain two thermo-responsive blocks, so two separate LCST behaviors was expected. The thermo-response of the aqueous state and corresponding LCSTSs of PDMAEMA and PNIPAM were detected by ^{1}H NMR analysis at variable temperature. (figure 9) At room temperature, the signals are assigned to PNIPAM block [(a, δ= 3.93 ppm) and (b, δ= 1.17 ppm)] and PDMAEMA block [(c, δ= 2.38 ppm), (d, δ= 4.23 ppm), (e, δ=2.84 ppm), and (f, δ= 0.97 ppm)]. The signal intensity of begins to decrease by the soluble-to-insoluble phase transition of each blocks.[22] For example, when the temperature increased to 40 ℃, PNIPAM peak of *a*, *b* become broad and decrease compared to room temperature, while main peak of PDMAEMA (*c*, *d*, *e*, and *f*) remained almost same. Similarly, when the temperature increased above 55 ℃, the signals attributed by PNIPAM block become almost flatten, and the signals attributed by PDMAEMA block start to disappear. To precisely compare the tendency of peak transition with monoblock polymer

(PD_{53}, PN_{40}), the intensity of typical signals (*a*, *e*) were normalized to their values at 30 ℃, and the results are summarized in figure 10.

As shown in figure 10, intensity of *a*_PN peak sharply decrease above 40 ℃ about 10% compared to 30 ℃, which is showing that PNIPAM undertaking soluble-insoluble phase transition at this temperature. In addition, intensity of *e*_PD peak continuously decrease from 40 ℃ to 60 ℃ until normalized integral decreases to 20%. Thus, we could deduce the LCST of $PNIPAM_{40}$ at about 40 ℃, and the LCST of $PDMAEMA_{53}$ at about 60 ℃. Furthermore, these tendency appears similarly at PDN block copolymer except that *e*_PDN peak decreases only until 55 ℃ unlike the *e*_PD peak. It demonstrates that PDN block copolymer has two LCST at about 40 ℃ and 55 ℃.

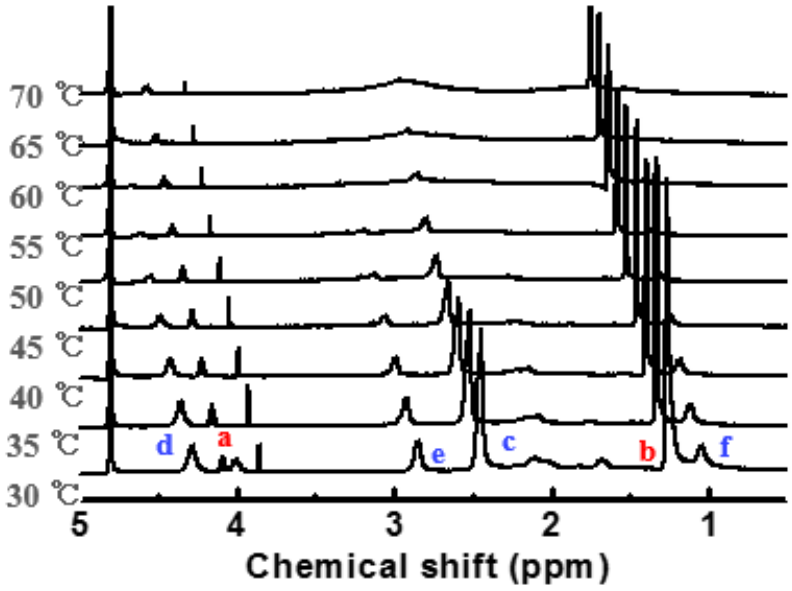

Figure 9. ^{1}H NMR spectra of PDN block copolymer (@D2O) at different temperature

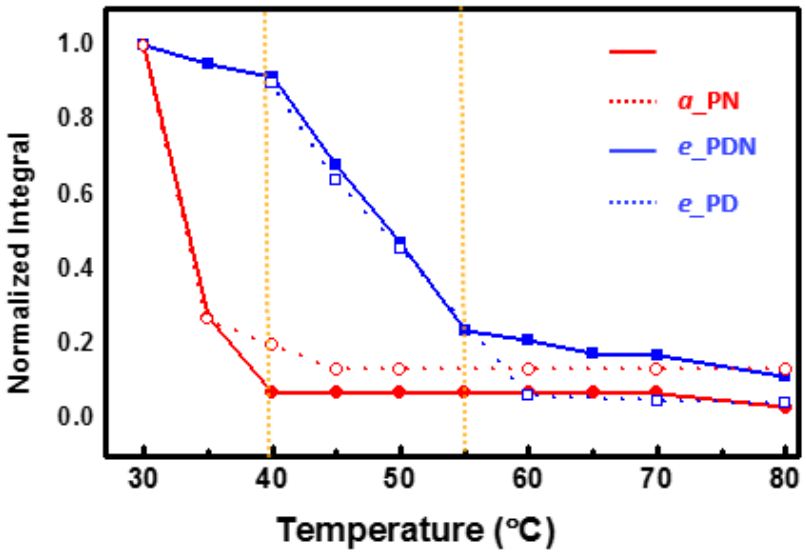

Figure 10. Normalized integral of ^{1}H NMR spectra at different temperature

3.2.2 Hydrodynamic size transition of PDN block copolymer

DLS analysis was performed to observe the hydrodynamic size transition of PDN block copolymer. As shown in figure 11, the hydrodynamic size was measured by DLS analysis. At initial state, PDN copolymers are dissolved in water, and no peaks were observed by DLS analysis. However, when the temperature increase above the 1st LCST (30-40 ℃) of PDN copolymers, PN blocks start to form coil-structure and aggregate each other because they are insoluble in water. Therefore, aggregated PDN copolymers begin to be recognized by DLS analyzer, and the size begins to increase due to the aggregation (a). And then, when the temperature increases above the 40 ℃, PD blocks also begin to shrink due to the solubility difference. Thus, the average size of aggregated PDN copolymer gradually decreases from 600 nm to 400 nm (b). Finally, if almost of the PD blocks are transited to coil-structure, the PDN block copolymer undergoes the 2nd aggregation which causes the dramatic increase of hydrodynamic size (c). The schematic diagram of each aggregations are illustrated in figure 11.

The final transition temperature of PD blocks appear as 70 ℃ which is generally increased value compared to ^{1}H NMR results. This is because that DLS analysis proceeds at dilute concentration (1 mg/mL) than ^{1}H NMR analysis (10 mg/mL) which makes the transition starts slowly at higher temperature. [31]

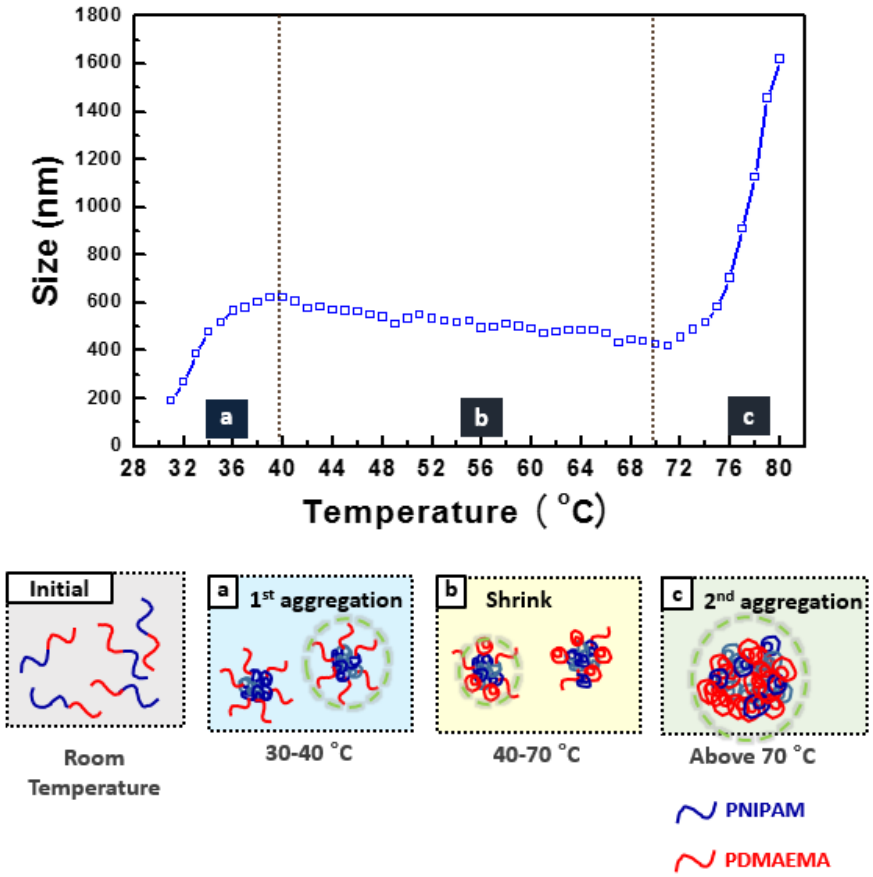

Figure 11. DLS results and schematic illustration of polymer transition

3.3. Characterization of PES/PDN membrane

3.3.1 Identification of PDN block copolymer in PES/PDN mebmrane

Figure 12 shows ATR-FTIR spectra of neat PES and PDN blended membrane surfaces prepared with different ratio of PDN copolymer. The peaks at 1486 cm^{-1} attributed to the stretching vibration of the S=O groups belonging to the sulfone groups. Additional peaks emerge at around 1740-1730 cm^{-1} and 1560-1540 cm^{-1} due to the carbonyl group of DMAEMA and amide group of NIPAM, thus confirming the presence of PDN block copolymer. The intensity of these peaks increased at PES/PDN10 which has higher amount of PDN compared to PDS/PDN5. In order to perform more quantitative analysis, peak intensity of carbonyl and amide group was normalized by comparing with peak intensity of S=O group. And normalized intensity corresponding with PDN concentration was appeared at figure 13. As expected, the normalized intensity of carbonyl and amide group increases proportional to the PDN concentration.

In order to identify the surface modification quantitatively, atomic concentration was observed by XPS analysis. As shown in the results at table 3, when PDN concentration increases on membrane surface, nitrogen concentration increases while sulfur concentration decreases.

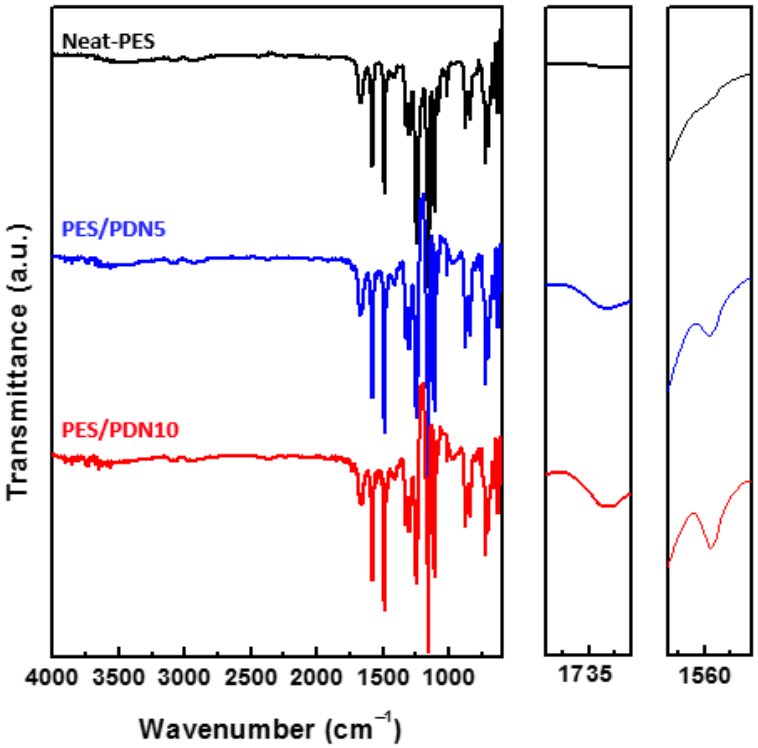

Figure 12. ATR/FT-IR spectra of Neat-PES, PES/PDN5 and PES/PDN10

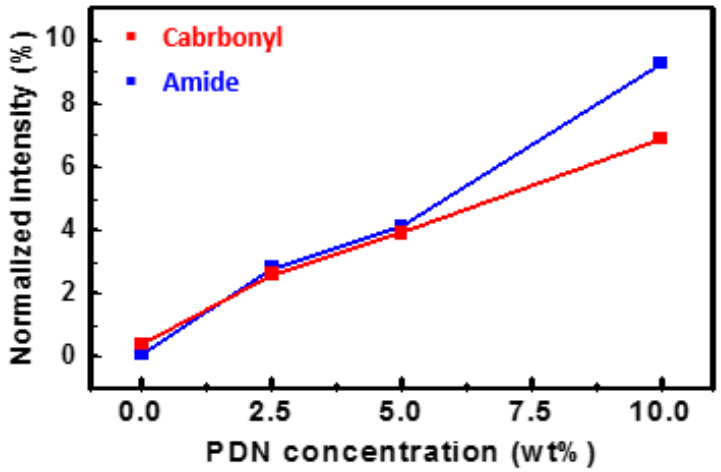

Figure 13. Normalized integral of carbonyl and amide peak related to PDN concentration

Table 3. Atomic concentration (%) of membranes analyzed by XPS

	Neat_PES	PES/PDN5	PES/PDN10
S_{2p}	3.54	3.33	3.12
C_{1s}	74.49	74.98	74.17
N_{1s}	**3.9**	**4.65**	**5.28**
O_{1s}	18.07	17.04	17.43

3.3.2 Membrane morphology and hydration capacity

The top surface and cross-section FESEM images of the neat PES membrane and the PDN blended membrane are shown at figure 14. It seems that PDN blended membrane (PES/PDN10) has higher pore density than neat PES membrane. This is because that hydrophilic segments of PDN block copolymer tends to form pore during coming out from the PES matrix. In case of the cross-sectional images, a typical asymmetrical structures which is composed of dense skin layer and finger-like sublayer are observed at all the membranes. Especially, PDN blended membrane has a larger and longer void in finger-like structure caused by the phase inversion of PDN block copolymers in water. Moreover, because the shrinkage which is occurred during the membrane formation is prevented by block copolymer, membrane is getting thicker after introduction of PDN block copolymer [36].

Hydration capacity of each membranes were determined and expressed in figure15. Usually hydration capacity is affected by porosity and hydrophilicity of membrane. When membrane has larger porosity, it can contain more water in it. Likewise, when membrane has higher hydrophilicity, it is easier to absorb water and hydration capacity might be increased. In order to exclude the effect of hydrophilicity, we wetted the membrane over than 12 hours. In case of neat-PES membrane, hydrophilicity and porosity does not change by the temperature transition, so hydration capacity is consistent regardless of temperature. On the other hand, both PES/PDN5 and PES/PDN10 membrane appears that the increase of hydration capacity at higher temperature. This is because that the thermo-responsible PDN block copolymer aggregates each other above the LCSTs, so the membrane porosity increases at higher temperature. Although the hydrophilicity decrease, hydration capacity of PES/PDN membrane increase at higher temperature as shown in figure 16 because porosity effect is stronger than hydrophilicity effect.

To discuss the approximate porosity variation of PES/PDN membrane at different temperature, we calculated porosity with following equation. Calculated porosity is shown at table 4.

$$\textbf{Porosity} = \frac{\text{Hydration capacity}[\text{mg/cm}^3]}{\text{Water density}[\text{mg/cm}^3]} \times 100 \qquad (4)$$

As expected, the porosity of neat-PES is almost same at each temperature, but the porosity of PES/PDN5 and PES/PDN10 membrane is increased about 1.2 times at each transition.

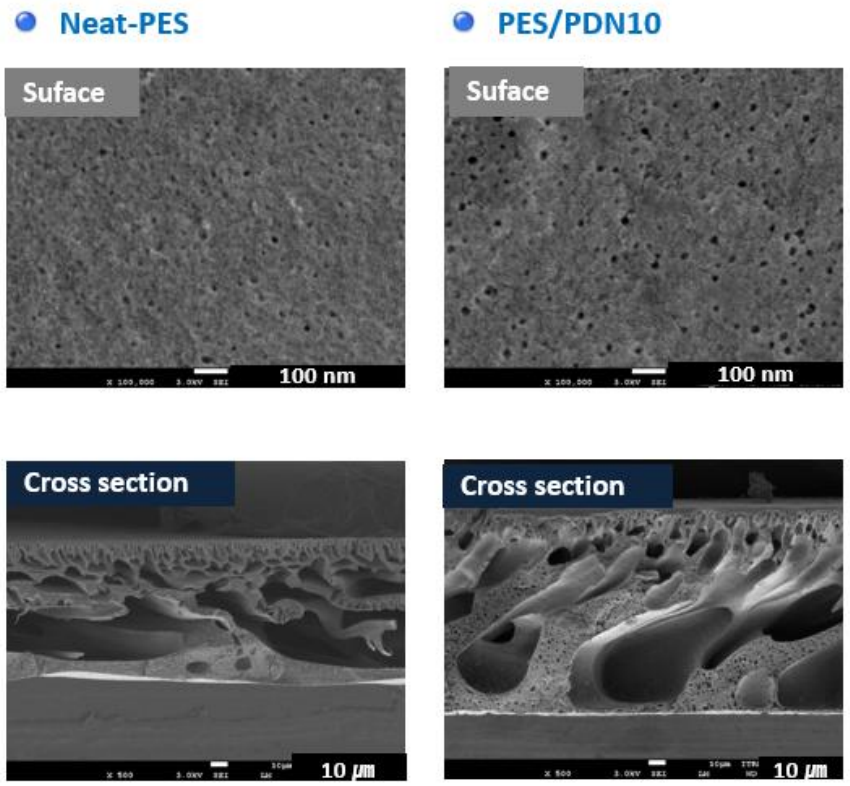

Figure 14. SEM images of neat-PES and PES/PDN 10 membrane (top: surface image, bottom: cross section image)

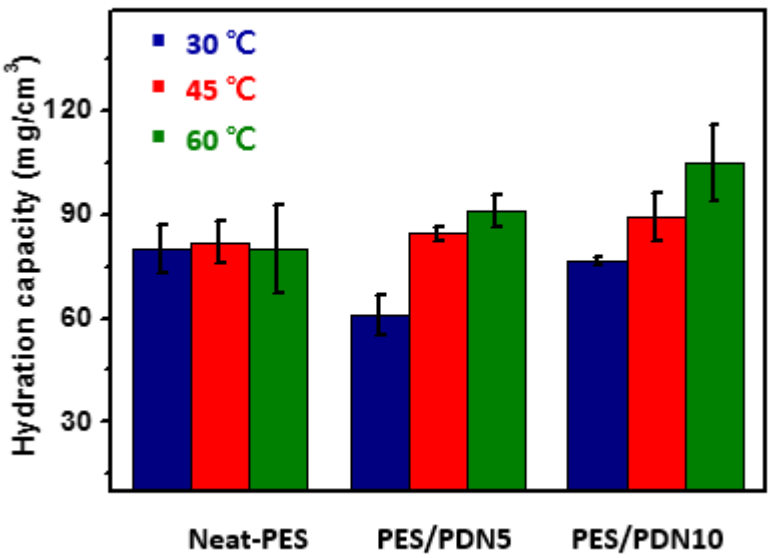

Figure 15. Average hydration capacity of neat-PES, PES/PDN5, and PES/PDN10

Table 4. Porosity transition of neat-PES, PES/PDN5, and PES/PDN10 at different temperature and schematic diagram for expected phenomenon

	30 ℃	45 ℃	60 ℃
Neat-PES	8.03 %	8.28 %	8.14 %
PES/PDN5	6.12 %	8.53 %	9.25 %
PES/PDN10	7.68 %	9.01 %	10.67 %
Diagram	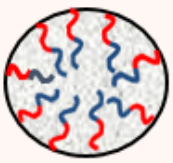	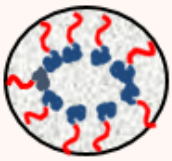	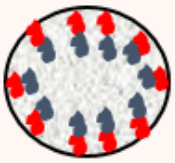

3.4. Filtration property

3.4.1 Pure water permeability

Figure 16 shows the pure water permeability of neat-PES membrane and PDN blended PES/PDN membranes. At room temperature, the water flux of the neat-PES membrane is the highest of all the prepared membrane, in spite of its dense structure which is observed by SEM images (figure 14). This is because that neat-PES membrane has better hydrophilicity than PES/PDN membranes. The contact angle was identified the hydrophilicity of each membranes. The PVP, the pore forming agent, has better hydrophilicity than PDN block copolymer, and neat-PES membrane has more PVP ratio than PES/PDN membranes because PES/PDN membrane contains PDN block copolymer instead of PVP.

This tendency keeps until 35 ℃ when the every block copolymers are stretched. Though, above 40 ℃, water flux of PES/PDN membranes begins to increase even though the neat-PES membrane shows the similar water flux regardless of the temperature change (1^{st} transition). Because solubility of PNIPAM blocks is changed and PNIPAM blocks near the pore aggregate each other, the porosity

increases. Therefore, water flux increases twice from 15 LMH to 30 LMH at both PES/PDN5 and PES/PDN10. Likewise, 2nd transition occurred at above 50 ℃. During the transition water flux of PES/PDN5 membrane increases from 30 LMH to 50 LMH. And in case of PES/PDN10 membrane, water flux increases from 36 LMH to 60 LMH. This transition is caused by change of PDMAEAM block to coil structure. Furthermore, this results are related with hydration capacity.

Following the same principles how porosity and hydrophilicity affects the hydration capacity, water flux is affected mainly by porosity. Therefore, we compared the water flux results with the porosity results. First of all, by the hagen-poiseuille (HP) model, water flux is proportional to square of pore diameter. At each transition, water flux increases about 1.7 times, so we can guess that the average pore diameter increases 1.3 times at each transition. The porosity which was calculated by hydration capacity results also show the similar tendency. As shown in table 4, the porosity increases 1.2 times at each transition. By the way, there are no significant difference between PES/PDN5 and PES/PDN10 regardless of the PDN concentration. Because the volume transition ratio of PDN is constant no matter the concentration, water flux changed with similar pattern in both PES/PDN5 and PES/PDN10.

Additionally we compare the transition temperature with the free PDN block copolymer's behavior. When the each polymers dissolved in water, transition of PNIPAM block occurred between 30 ℃ to 40 ℃ and transition of PDMAEMA block occurred between 40 ℃ to 60 ℃ (in case of the ^{1}H NMR results). Otherwise, when the polymers are embedded in the membrane matrix, transition occurred at higher temperature. Since free polymers move more easily than stuck polymers, transition occurs more slowly in case of membrane. Thus, overall transition temperature increases at water filtration tests compared with ^{1}H NMR and DLS results.

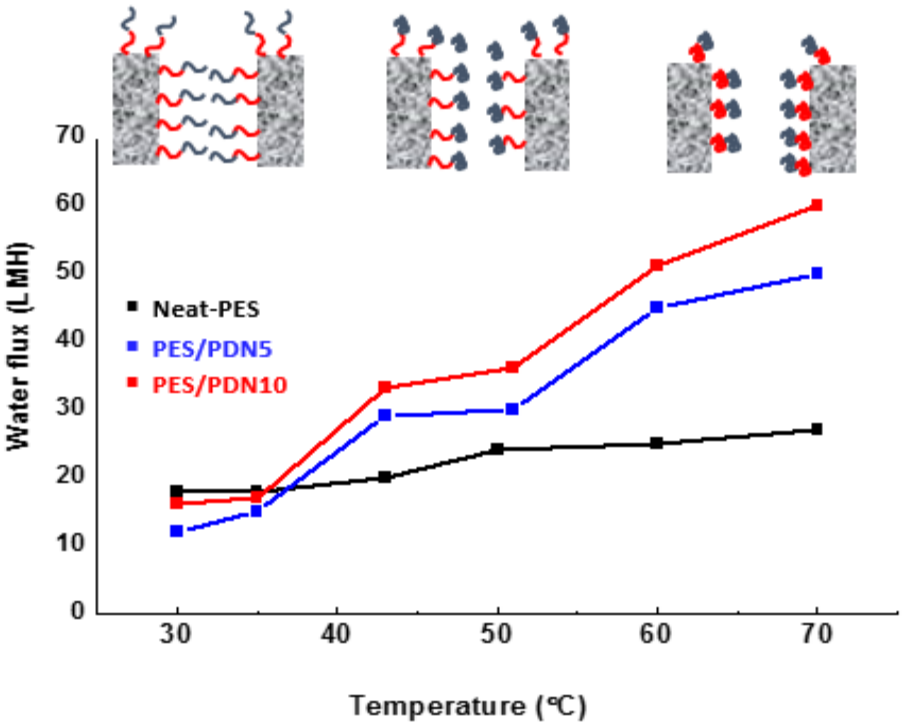

Figure 16. Pure water filtration transition at different temperature of neat-PES, PES/PDN5, and PES/PDN10

3.4.2 Permeation ratio of proteins

The size of filtered materials becomes different according to the membrane pore size. Thus, we measured the permeation ratio of 3 different proteins (Lysozyme: 14 kDa, BSA: 66 kDa, Globulin: 92 kDa) with neat-PES, PES/PDN5, and PES/PDN10 membranes in order to observe the transition of pore size (figure 17). At preferentially we compare the permeation ratio at room temperature.

As expected, lysozyme (which has smallest molecular weights among three proteins) permeates the most. BSA molecules are permeated only about 10 % and globulin molecules are scarcely found in permeated solution. Thus, these proteins are suitable for estimate the pore size transition according to temperature change. At first, neat-PES membrane shows similar permeation ratio across the whole temperature range. It means that temperature doesn't affect the pore size of neat-PES. Even though there is slight decrease of lysozyme permeation ratio, it is an observational error came out by the difference of membrane. On the other hand, permeation ratio increases at PES/PDN5 and PES/PDN10 membranes. In detail, most of lysozyme molecules permeate through membrane above 50 ℃ both PES/PDN5 and PES/PDN10 despite their

permeation ratio is only about 20-30 % at lower temperature. Likewise, permeation ratio of BSA molecules dramatically increase when the temperature increases to 60 ℃. Globulin molecules are too large to permeate through the membrane, so the permeation ratio is still below 20 % at 70 ℃. Permeation ratio of both lysozyme molecules and BSA molecules increase more dramatically at PES/PDN10 membrane than PES/PDN5 membrane.

The schematic illustration of how the prepared two step thermo-responsive membrane permeates the different molecules is shown in figure 18. First of all, at lower temperature (30-40 ℃), only small molecules could permeate the pore due to the small pore size. Thus, some parts of lysozyme permeate the membrane (a). And then, when the temperature increases to 40-50 ℃, membrane pore expands large enough to permeate almost of lysozyme molecules but not enough to permeate BSA and globulin molecules (b). Finally, when the temperature increases further until PDMAEMA blocks could shrink, BSA molecules also are able to pass through the membrane. However, still globulin molecules are too large to pass through the membrane (c). Consequently, with the permeation experiments we proved that different solutes could be separated respectively by the temperature

transition.

In addition, we try to calculate the average pore size by the permeation ratio results. According to the sarbolouki, solute retention ratio (SR %) of particular molecules is related to size of membrane pore and filtered molecules. Therefore, they express the relationship of SR % and pore size as equation (5).

$$\mathbf{SR}\ \% = \frac{\bar{a}}{R} \times 100 \tag{5}$$

SR % is solute retention ratio, $\bar{a}$ is radius of permeated solute, and $\overline{R}$ is average pore radius of membrane [37, 38].

Solute retention ratio means the concentration of rejected solute, and it could be obtained as the opposite value of permeation ratio. Furthermore, this equation can be applied only if the solute retention ratio is above 80 %. In this research, the membrane pore radius could be taken using permeation ratio of BSA molecules and globulin molecules. The average solute radius of BSA molecules and globulin molecules are known as 37 Å and 46 Å. The average pore size at 30-50 ℃ was calculated by permeation ratio of BSA because their SR % is below the 80 % at higher temperature. And average pore size at 60-

70 ℃ was calculated by permeation ratio of globulin. The results were expressed as table 5. At room temperature, membrane pore size is determined about 44-46 Å. In addition, pore size increases about 1.15 times at each transition. Therefore, this results mean that pore size increases with the temperature increases, and it could affect the permeation ratio of proteins.

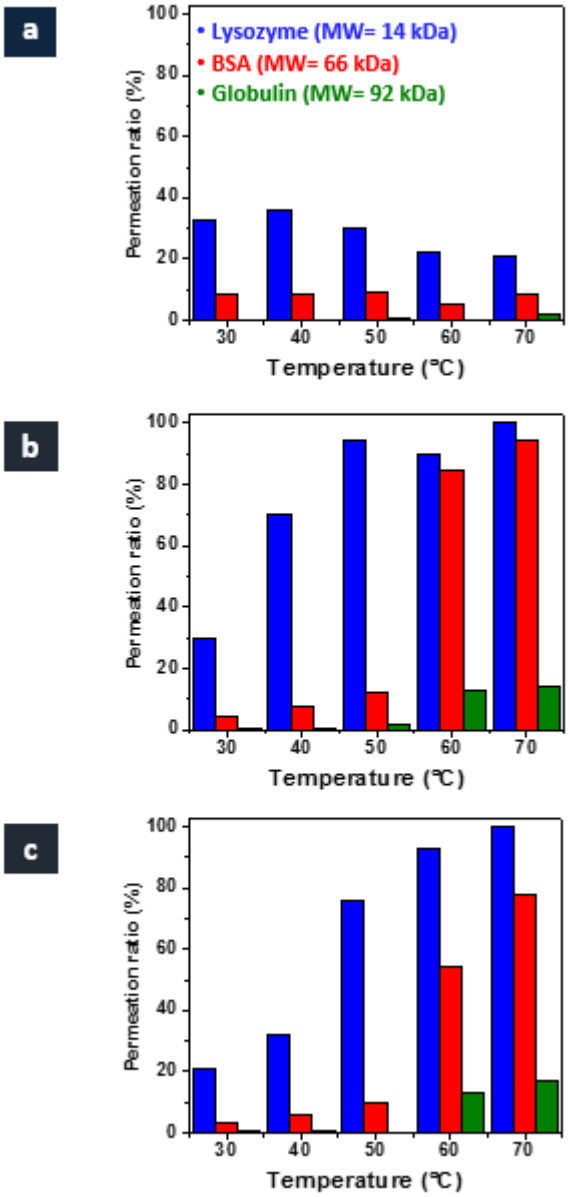

Figure 17. Permeation ratio of three different proteins (lysozyme, BSA, globulin) (a : neat-PES, b : PES/PDN5, c : PES/PDN10)

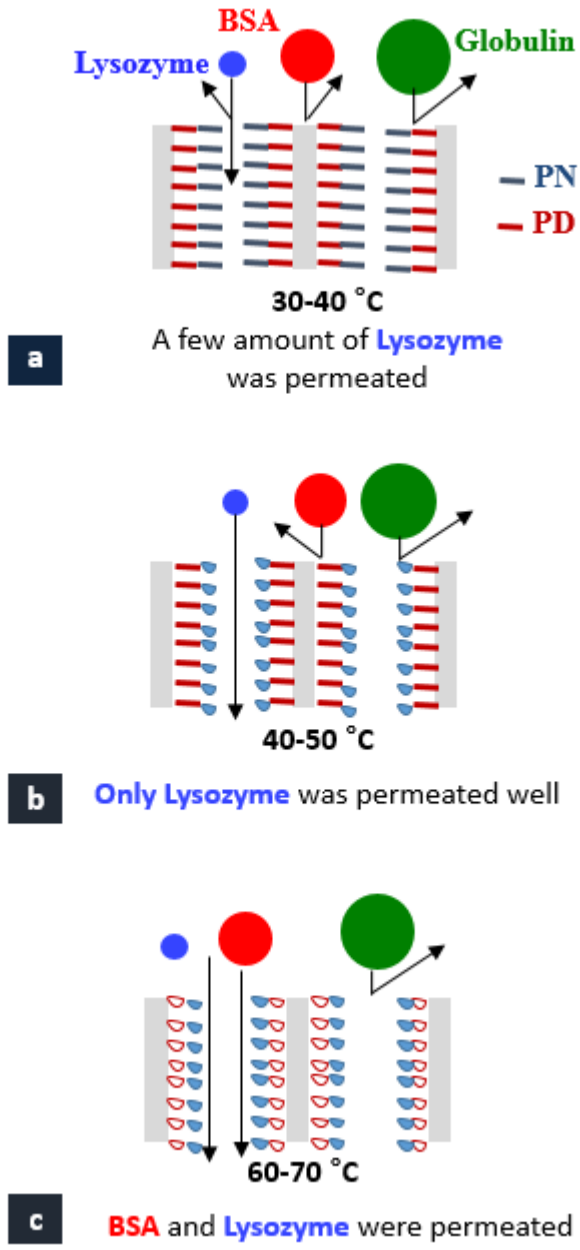

Figure 18. Schematic diagrams for protein separation (a : 30-40 °C, b : 40-50 °C, c : 60-70 °C)

Table 5. Pore size transition of neat-PES, PES/PDN5, and PES/PDN10

	Neat-PES	PES/PDN5	PES/PDN10
30 ℃	46.3	44.6	44.0
40 ℃	46.3	46.4	45.1
50 ℃	46.7	51.2	49.3
60 ℃	44.7	56.3	56.3
70 ℃	46.3	58.0	58.8

3.5. Cleaning performance

Fouling tests were performed with hemoglobin solution. Hemoglobin has molecular weight of 64 kDa which is similar to BSA molecules, so it could be rejected by the membrane well at low temperature but could permeate the membrane at higher temperature. Also, hemoglobin has neutral charge which cannot affect electrostatic repulsion. The filtration results are normalized as the initial flux, and final results are expressed in figure 19.

The water flux dramatically decreases after permeating the hemoglobin solution since membrane surface is contaminated by hemoglobin molecules. As shown in figure 19, neat-PES fouled the most compared to PES/PDN membrane. When pure water flux were observed again after washing the membrane at 30 ℃ and 60 ℃ respectively, water flux slightly recovered. However, in case of neat-PES shows a little recovery compared to PES/PDN membrane. It means that PDN block copolymer has a fouling resistance property.

Also, neat-PES membrane shows similar recovery property by the temperature. Otherwise, in case of PES/PDN membrane flux recovered more at 60 ℃ than 30 ℃. This is because hemoglobin molecules are detached from membrane more easily when the polymers are aggregated by large pore size and physical elution. Furthermore, PES/PDN10 shows better flux recovery than PES/PDN5 membrane because PES/PDN10 has more PDN polymers near the pore and surface and it makes hemoglobin molecules be detached more easily.

To discuss the flux recovery property with the specific values, we calculated the flux recovery ratio and reversible/irreversible fouling resistance by the following equation:

$$\mathbf{FRR}\ (\%) = \frac{J_R}{J_0} \times 100 \tag{6}$$

$$\mathbf{R}_r = \frac{J_R - J_P}{J_0} \times 100 \tag{7}$$

$$\mathbf{R}_{ir} = \frac{J_0 - J_R}{J_0} \times 100 \tag{8}$$

Neat-PES shows the similar FRR % at both temperature, but PES/PDN membranes show the increased FRR % values at high temperature. It demonstrates that cleaning efficiency is improved at high temperature in case of PES/PDN membrane.

Also, R_{ir} (irreversible fouling resistance) is dominant value at neat-PES, but PES/PDN membrane show relatively higher values at R_r (reversible fouling resistance). Therefore, PES/PDN membranes could be recovered reversibly than neat-PES membrane. Furthermore, it could be used for a long cycle without a chemical cleaning compared to ordinary membrane.

Especially, FRR % and R_r increase more at PES/PDN10 membrane than PES/PDN5 membrane though both membrane show the similar performance at filtration tests. PDN concentration did not affect the porosity and pore size because every polymers show comparable volume transition rates. Otherwise, PDN concentration has an effect on cleaning efficiency because total volume transition power increases and therefore absorbed molecules are easily detached.

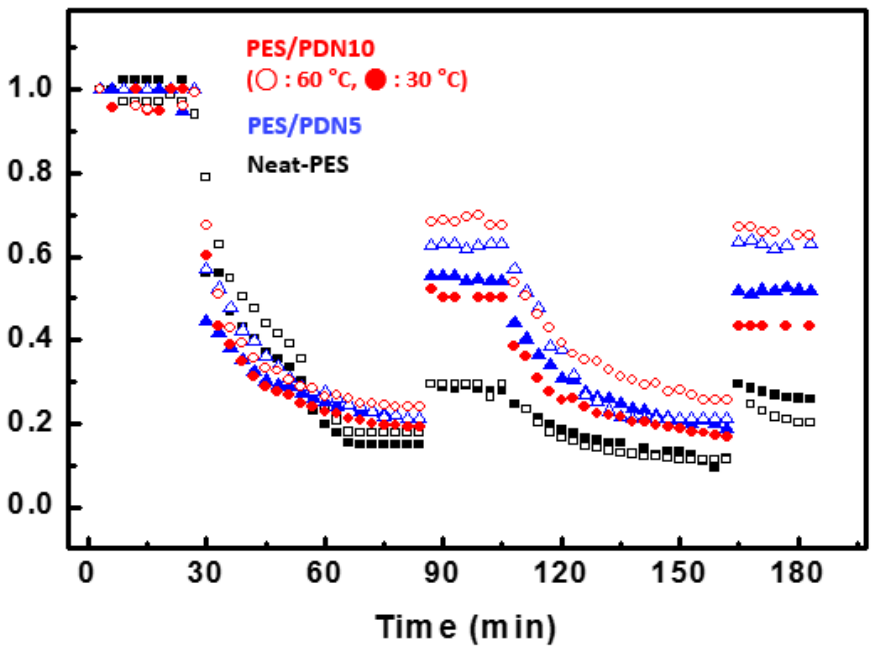

Figure19. Fouling test results of neat-PES (■), PES/PDN5 (▲), and PES/PDN10 (●).
■(filled): cleaning at 30 ˚C, □(blanked): cleaning at 60 ˚C

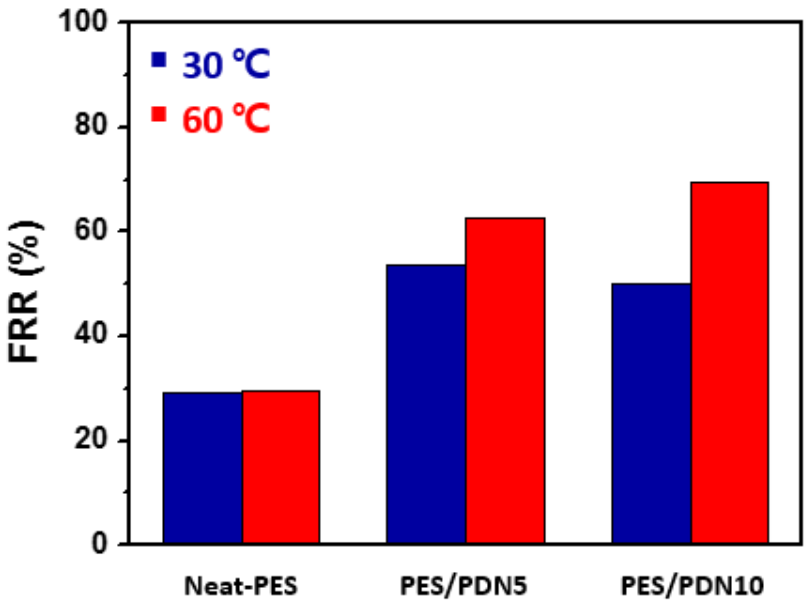

Figure 20. FRR% (Flux recovery ratio) of neat-PES, PES/PDN5, and PES/PDN10

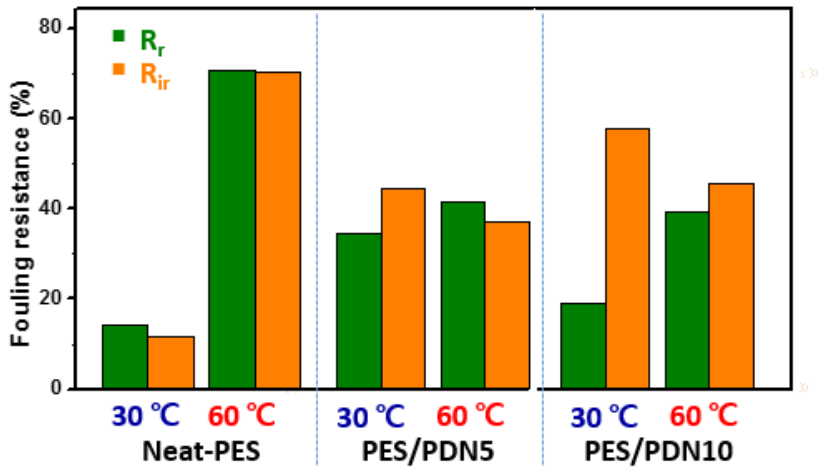

Figure 21. Reversible/Irreversible fouling resistance of neat-PES, PES/PDN5, and PES/PDN10

Table 6. Transition temperature range of PDN polymer and PES/PDN membrane

	1st Transition	2nd Transition
PDN polymer	30-40 °C	40-60 °C
PES/PDN membrane	35-45 °C	50-70 °C

4. Conclusion

In this research, we prepared two step thermo-responsive membrane in order to present tunable separation property and improved cleaning efficiency. Initially, NIPAM which have LCST behavior at room temperature region and DMAEMA which can change the LCST temperature according to the molecular weight were polymerized as PDN block copolymer (PDMAEMA-b-PNIPAM) by RAFT polymerization. And then, synthesized polymers were blended with PES, and PES/PDN membrane was prepared by phase inversion method.

FT-IR and ^{1}H NMR analysis identified the successful polymerization of PDN block copolymer. And by the ^{1}H NMR and DLS analysis at D_2O solution, we confirmed that PNIPAM block aggregates above 40 ℃ and PDMAEMA block aggregates during 40-60 ℃. The difference of transition temperature is caused from the concentration difference of each analyze. Next, we confirmed that PDN is successfully blended with PES membrane without a significant change of its morphology. Hydration capacity results proved that PES/PDN membrane can contain more water at high temperature in

spite of the hydrophilicity. Then, porosity which was calculated by hydration capacity increases with the temperature increase, and these results are related with water flux transition of each membrane. Permeation ratio of three different proteins (lysozyme, BSA, globulin) proved that tunable separation property of prepared membrane. According to the temperature increases larger molecules could pass through the membrane. Finally, cleaning efficiency was determined by fouling tests. And PES/PDN membranes show better fouling resistance compared to neat-PES. Furthermore, when cleaning the PES/PDN membrane at higher temperature, flux recovery ratio increases from 50 % to 65-70 %. Concentration of PDN block copolymers did not affect to the porosity and pore size of membrane. Otherwise, cleaning efficiency improved when membrane has more PDN concentration. Overall transition temperature at PES/PDN membrane was increased compared to PDN block copolymer's transition temperature (table 6).

As a result, PES/PDN membrane shows two step thermo-responsibility, and it shows tunable separation property and improved cleaning efficiency. Therefore, it could be used at separation application such as protein separation and process food molecules. Also it could be used for a long cycle without a chemical cleaning due to the

improved cleaning efficiency.

5. Reference

[1] Kang, Guo-dong, and Yi-ming Cao. "Application and modification of poly (vinylidene fluoride)(PVDF) membranes–A review." *Journal of Membrane Science* 463 (2014): 145-165.

[2] Mohammad, Abdul Wahab, et al. "Ultrafiltration in food processing industry: review on application, membrane fouling, and fouling control." *Food and bioprocess technology* 5.4 (2012): 1143-1156.

[3] Madaeni, S. S., S. Zinadini, and V. Vatanpour. "A new approach to improve antifouling property of PVDF membrane using in situ polymerization of PAA functionalized TiO 2 nanoparticles." *Journal of Membrane Science* 380.1 (2011): 155-162.

[4] Shi, Xiafu, et al. "Fouling and cleaning of ultrafiltration membranes: a review."*Journal of Water Process Engineering* 1 (2014): 121-138.

[5] Yang, Sung Yun, and Michael F. Rubner. "Micropatterning of polymer thin films with pH-sensitive and cross-linkable hydrogen-bonded polyelectrolyte multilayers." *Journal of the American Chemical Society* 124.10 (2002): 2100-2101.

[6] Xiao, Li, et al. "Development of bench and full-scale temperature

and pH responsive functionalized PVDF membranes with tunable properties." *Journal of membrane science* 457 (2014): 39-49.

[7] Yang, Qian, et al. "Designing magnetic field responsive nanofiltration membranes." *Journal of membrane Science* 430 (2013): 70-78.

[8] Zhao, Yong-Hong, Kin-Ho Wee, and Renbi Bai. "A novel electrolyte-responsive membrane with tunable permeation selectivity for protein purification." *ACS applied materials & interfaces* 2.1 (2009): 203-211.

[9] Wang, Guan, et al. "Thermo-Responsive Polyethersulfone Composite Membranes Blended with Poly (N-isopropylacrylamide) Nanogels." *Chemical Engineering & Technology* 35.11 (2012): 2015-2022.

[10] Schattling, Philipp, Florian D. Jochum, and Patrick Theato. "Multi-stimuli responsive polymers–the all-in-one talents." *Polymer Chemistry* 5.1 (2014): 25-36.

[11] Stuart, Martien A. Cohen, et al. "Emerging applications of stimuli-responsive polymer materials." *Nature materials* 9.2 (2010): 101-113.

[12] Wandera, Daniel, S. Ranil Wickramasinghe, and Scott M. Husson.

"Stimuli-responsive membranes." *Journal of Membrane Science* 357.1 (2010): 6-35.

[13] Kratz, Karl, Thomas Hellweg, and Wolfgang Eimer. "Structural changes in PNIPAM microgel particles as seen by SANS, DLS, and EM techniques."*Polymer* 42.15 (2001): 6631-6639.

[14] Chen, J. J., A. L. Ahmad, and B. S. Ooi. "Thermo-responsive properties of poly (N-isopropylacrylamide-co-acrylic acid) hydrogel and its effect on copper ion removal and fouling of polymer-enhanced ultrafiltration." *Journal of Membrane Science* 469 (2014): 73-79.

[15] Yang, Mei, et al. "Gating characteristics of thermo-responsive and molecular-recognizable membranes based on poly (N-isopropylacrylamide) and β-cyclodextrin." *Journal of Membrane Science* 355.1 (2010): 142-150.

[16] Hu, Lin, et al. "A Composite Thermo-Responsive Membrane System for Improved Controlled-Release." *Chemical engineering & technology* 30.4 (2007): 523-529.

[17] Nash, Maria E., et al. "Cell and cell sheet recovery from pNIPAm

coatings; motivation and history to present day approaches." *Journal of Materials Chemistry* 22.37 (2012): 19376-19389.

[18] Yu, Jing-Zhen, et al. "Poly (N-isopropylacrylamide) grafted poly (vinylidene fluoride) copolymers for temperature-sensitive membranes." *Journal of Membrane Science* 366.1 (2011): 176-183.

[19] Chen, Xi, et al. "Temperature-sensitive membranes prepared from blends of poly (vinylidene fluoride) and poly (N-isopropylacrylamides) microgels." *Colloid and Polymer Science* 291.10 (2013): 2419-2428.

[20] Li, Qian, et al. "A novel ultrafiltration (UF) membrane with controllable selectivity for protein separation." *Journal of Membrane Science* 427 (2013): 155-167.

[21] Yu, Sanchuan, et al. "Surface modification of thin-film composite polyamide reverse osmosis membranes by coating N-isopropylacrylamide-co-acrylic acid copolymers for improved membrane properties." *Journal of membrane science*371.1 (2011): 293-306.

[22] Hsu, Che-Chuan, Chuan-Shao Wu, and Ying-Ling Liu. "Multiple

stimuli-responsive poly (vinylidene fluoride) (PVDF) membrane exhibiting high efficiency of membrane clean in protein separation." *Journal of Membrane Science* 450 (2014): 257-264.

[23] Sinha, M. K., and M. K. Purkait. "Preparation of a novel thermo responsive PSF membrane, with cross linked PVCL-co-PSF copolymer for protein separation and easy cleaning." *RSC Advances* 5.29 (2015): 22609-22619.

[24] Zhou, Shouyong, et al. "Fabrication of temperature-responsive ZrO 2 tubular membranes, grafted with poly (N-isopropylacrylamide) brush chains, for protein removal and easy cleaning." *Journal of Membrane Science* 450 (2014): 351-361.

[25] Weiss, Jan, Christoph Böttcher, and André Laschewsky. "Self-assembly of double thermoresponsive block copolymers end-capped with complementary trimethylsilyl groups." *Soft Matter* 7.2 (2011): 483-492.

[26] Li, Quanlong, et al. "Doubly thermo-responsive nanoparticles constructed with two diblock copolymers prepared through the two macro-RAFT agents co-mediated dispersion RAFT polymerization." *Polymer Chemistry* 6.1 (2015): 70-78.

[27] Pietsch, Christian, et al. "Thermo-induced self-assembly of responsive poly (DMAEMA-b-DEGMA) block copolymers into multi- and unilamellar vesicles."*Macromolecules* 45.23 (2012): 9292-9302.

[28] Wei, Hua, et al. "One-pot ATRP synthesis of a triple hydrophilic block copolymer with dual LCSTs and its thermo-induced association behavior." *Soft Matter* 8.37 (2012): 9526-9528.

[29] Weiss, Jan, Christoph Böttcher, and André Laschewsky. "Self-assembly of double thermoresponsive block copolymers end-capped with complementary trimethylsilyl groups." *Soft Matter* 7.2 (2011): 483-492.

[30] Furyk, Steven, et al. "Effects of end group polarity and molecular weight on the lower critical solution temperature of poly (N-isopropylacrylamide)." *Journal of Polymer Science Part A: Polymer Chemistry* 44.4 (2006): 1492-1501.

[31] Han, Xia, et al. "Effect of composition of PDMAEMA-b-PAA block copolymers on their pH-and temperature-responsive behaviors." *Langmuir* 29.4 (2013): 1024-1034.

[32] Moad, Graeme, et al. "Advances in RAFT polymerization: the synthesis of polymers with defined end-groups." *Polymer* 46.19 (2005): 8458-8468.

[33] Li, Quanlong, et al. "Doubly thermo-responsive ABC triblock copolymer nanoparticles prepared through dispersion RAFT polymerization." *Polymer Chemistry* 5.8 (2014): 2961-2972.

[34] Luo, Tao, et al. "pH-responsive poly (ether sulfone) composite membranes blended with amphiphilic polystyrene-block-poly (acrylic acid) copolymers."*Journal of Membrane Science* 450 (2014): 162-173.

[35] Ismail, Ahmad Fauzi, and Abdul Rahman Hassan. "Effect of additive contents on the performances and structural properties of asymmetric polyethersulfone (PES) nanofiltration membranes." *Separation and purification technology* 55.1 (2007): 98-109.

[36] Venault, Antoine, et al. "Low-biofouling membranes prepared by liquid-induced phase separation of the PVDF/polystyrene-b-poly (ethylene glycol) methacrylate blend." *Journal of Membrane Science* 450 (2014): 340-350.

[37] Sarbolouki, M. N. "A general diagram for estimating pore size of ultrafiltration and reverse osmosis membranes." *Separation Science and Technology* 17.2 (1982): 381-386.

[38] Sarbolouki, Mohammad N. "Properties of asymmetric polyimide ultrafiltration membranes. I. Pore size and morphology characterization." *Journal of applied polymer science* 29.3 (1984): 743-753.

[39] Dimitrov, Ivaylo, et al. "Thermosensitive water-soluble copolymers with doubly responsive reversibly interacting entities." *Progress in Polymer Science* 32.11 (2007): 1275-1343.

국문초록

Ultra/micro filtration (UF/MF) 분리막은 다른 수처리 공정보다 쉽고 간단하다는 장점을 갖고 있어 널리 활용되고 있다. 그러나 분리막을 이용한 공정은 한번 설계된 구조에 의해 그 성능이 제한된다는 점과, 단백질과 같은 유기물질에 의해 쉽게 오염될 수 있다는 한계를 갖고 있다. 이번 연구에서는 열 감응성 블록 고분자를 도입함으로써 두 단계로 분리성능이 조절되고 세척효율이 향상되는 분리막을 제조해보았다. 이를 위하여 먼저 서로 다른 두 개의 LCST 거동을 갖는 폴리디메마-b-폴리나이팜 (PDMAEMA-b-PNIPAM, PDN) 블록 고분자를 합성하였다. 그리고, 이를 폴리설폰 막 재료와 섞어 주어 상전이 방법을 이용하여 분리막을 제조하였다. 적외선 분광광도계 (FT-IR) 분석과 핵자기 공명 분광 (^{1}H NMR) 분석을 통해, 고분자 중합이 성공적으로 이루어졌음을 확인하였다. 또한, 수상 조건에서의 핵자기 공명 분광 (^{1}H NMR) 분석과 동적 광산란 (DLS) 분석을 통하여 중합된 고분자의 LCST가 각각 40 °C와 40-60 °C 조건에서 나타남을 확인할 수 있었다. 감쇠 전반사 적외선 분광광도계 (ATR/FT-IR) 분석 및 광전자 분광기 (XPS) 분석을 실시하여 중합된 고분자가 분리막의 구조를 크게 변화시키지 않으면서 내부에 잘 도입되었음을 확인하였다. 마지막으로 분리막이 두 단계로 분리성능이 조절되고 세척효율이 향상되었는지 확인하기 위하여, 투과도 실험과 오염저감도 실험이 진행되었다. 예상했던대로 PDN이 도입된 PES/PDN 분리막의 경우 40 °C와 50-70 °C에서 각각 수투과도 및 단백질들의

투과율이 증가하는 것을 확인할 수 있었다. 또한, 오염된 막을 세척하였을 때도 세척 효율이 60 °C에서 세척하였을 때가 30 °C에서 세척하였을 때보다 더 증가하는 것을 확인할 수 있었다. 이를 통하여 두 단계로 온도에 반응하여 분리성능을 조절하고 세척효율도 향상되는 분리막을 성공적으로 제조하였고, 이를 이용하여 한 가지의 막으로 다양한 단백질들을 분리할 수 있으며 오염에 대한 저항성도 키울 수 있음을 확인하였다.

감사의 글

2년여 간의 석사과정 동안 무사히 제 연구를 마치고 졸업을 할 수 있게 도와주신 많은 분들께 감사의 인사를 드리고자 합니다.

먼저 2년 동안 좋은 연구환경을 제공해주시고, 연구가 나아가야 할 방향성에 대해 조언해주신 곽승엽 지도교수님께 진심으로 감사 드립니다. 바쁘신 가운데 학위논문 심사에 자리해 주신 안철희 교수님께도 감사 드립니다. 또한, 저의 연구에 대해 지속적으로 관심을 갖고 연구 내외적인 면에서 많은 조언을 주셨으며 마지막 학위논문 심사까지 자리해주신 정재우 교수님께도 감사의 마음을 전합니다.

2년 동안 저와 가장 많은 시간을 보내며 많은 힘이 되어주셨던 연구실 선후배들에게도 감사의 인사를 전하고자 합니다. 연구실 생활 중 어렵거나 힘든 일이 있을 때 언제나 다정하게 격려해주신 저희 연구실의 리더 수열오빠, 모든 사람들의 별명을 하나하나 붙여주시며 관심 가져주는 현중오빠, 연구 주제 선정부터 실험 설계까지 제 연구의 기반이 되는 전반적인 것에 많은 도움을 주신 성용오빠, 말로는 표현할 수 없으나 누구보다도 연구에 대한 열정과 속정이 깊으신 우혁오빠, 2년 동안 사용할 피피티 템플릿의 제공자이자 연구실 생활의 대소사에 많은 조언을 해주신 지훈오빠, 실험 결과와 발표에 대해 저보다 더 열심히 관심 갖고 조언해주시며 옆 자리에서 든든히 저를 도와주셨던 제 사수 태선오빠, 연구실의 귀염둥이이자 만물박사를 맡고 있으며 실험할 때 이런저런 많은 조언을 해주신 지환오빠, 낯은 가리지만 친해지면 누구보다도 말 많고

웃긴 규원오빠, 연구부터 발표까지 무엇이든 잘 해내는 멋진 용준오빠, 항상 성실한 준호오빠, 언제나 허허 웃으며 어린 동생들의 짓궂은 농담까지도 받아주시는 강하지만 착한 승환오빠, 늦게 들어오셔서 많은 이야기를 나누진 못했지만 사람 좋으신 준형오빠, 궂은일 먼저 도맡아 해주며 힘들 때 힘이 되어주고 같이 응원해줄 수 있는 버팀목이 되어줬던 내 동기 용규오빠, 언제나 낙천적이고 즐거운 실험실 긍정마스코트 승택오빠, 여자인 저보다 여리여리한 몸으로 반전의 모습을 선사하던 대연이, 너무 엉뚱해서 답답하기도 하지만 속은 여리고 착한 성우까지 모두 감사 드립니다. 그리고 석사 첫 1년 동안 같은 여자라고 많이 아껴주고 도와주던 졸업한 선배 예지언니에게도 감사 인사 전합니다.

마지막으로 매일 늦게 퇴근하는 딸의 온갖 짜증 다 받아주시며 격려해주신 우리 부모님, 먼 곳에서 서로를 응원하며 힘낼 수 있게 도와준 나의 가장 소중한 동생 정수, 졸업 심사 직전에 좋은 곳으로 떠나셔서 흐뭇하게 저를 지켜보고 계실 보고 싶은 우리 외할머니께도 감사 드립니다.

사회에 나가서도 연구실에서 배운 지식과 경험을 바탕으로 더 나은 인재가 될 수 있도록 노력하겠습니다. 2년 동안 진심으로 감사했습니다.